PHYSICAL REVIEW B VOLUME 15, NUMBER 8 15 APRIL 1977

Phonons in AX_2 glasses: From molecular to band-like modes

P. N. Sen* and M. F. Thorpe†
Xerox Palo Alto Research Center, Palo Alto, California 94304
(Received 20 September 1976)

We study the vibrational density of states of glassy AX_2 systems such as SiO_2 and GeS_2 which consist of tetrahedra linked together to form a random network. We show that the higher-frequency modes can be well represented by a model with a single-nearest-neighbor central force. This model leads to an isomorphism of the vibrational modes to the electronic properties of the tetrahedral network studied by Weaire and Thorpe. This allows us to study the metamorphosis of the vibrational modes from molecular-like to band-like as a function of the AXA bond angle and the masses. The spectral limits delineating the allowed frequency regions and the character of the modes are found. These are independent of the detailed nature of the random network. The effect of a noncentral force is considered for the two extreme limits of AXA bond angles (i.e., 90° and 180°). We conclude that it is justified to consider an amorphous network as an assembly of weakly interacting molecular units when the AXA bond angle is close to 90° and the angular forces are weak. We classify BeF_2, GeS_2, and $GeSe_2$ as being dominated by molecular effects, whereas the solid-state effects are most important in SiO_2 and GeO_2.

I. INTRODUCTION

Although a good deal of experimental data is now available[1] on amorphous materials, particularly semiconductors, our theoretical understanding of the vibrational properties of random networks is much less complete than it is for crystals. This is because the lack of microscopic translational invariance prevents the vibrational excitations being described in terms of plane waves propagating from unit cell to unit cell.

The principal theoretical approaches used to date have involved either numerical techniques to determine the modes of random networks[2,3] or attempts to identify molecular units that retain their integrity to some degree in the amorphous solid.[4] Numerical techniques have been applied to SiO_2 networks[2] and Si networks.[3] The AX_2 glasses, of which SiO_2 is a prototype, are generally believed to be continuous random networks of nearly perfect AX_4 tetrahedra.[5] These networks can be hand-built and typically contain ~500 molecular units. The problem is then reduced to one of diagonalizing a large matrix and finding the associated density of eigenvalues. Some special techniques have been developed for handling such problems, but there is ultimately a limitation in that only a finite piece of network can be handled. With care over the treatment of the surface, rather good density of states have been obtained (good in the sense that they are representative of the infinite network). The results show that amorphous Si is best regarded as a giant covalently bonded molecule and cannot be subdivided into molecular units in any obvious way. This is also true in SiO_2, where the density of states is broad and does not contain any sharp features as would be expected if it could be decomposed into weakly interacting molcular units.

On the other hand, Lucovsky and co-workers[1,4] have had considerable success in interpreting the spectra of the chalcogenide glasses (As_2Se_3, GeS_2, etc) in terms of molceular modes. Indeed, the experimental spectra do show sharp features in contrast to Si and SiO_2, where broad bands are observed.

In previous work,[6] we have shown that the spectrum of Si can be understood in terms of a five-atom tetrahedron of Si atoms embedded in an effective homogeneous medium whose properties are determined so that all five atoms vibrate isotropically with the same amplitude. However, it was found that the resulting density of states bore little resemblance to the "molecular modes" of the isolated tetrahedron—that is, the coupling to the rest of the network was strong.

This work was extended to SiO_2 by including four O atoms midway between the central Si and the outer four Si atoms[7] so that Si–O–Si formed a straight bond. The straight bond used as the basic unit had high symmetry that facilitated calculation. Although the resulting spectrum contained both sharp features and extended structure, it was again concluded that the modes of an isolated SiO_4 tetrahedron gave little indication about the position of the sharp features in the network. The reason for this is clear. By far the strongest force in the problem is the nearest-neighbor central force; and while a O experiences only a single force from the Si in the SiO_4 molecule, it experiences forces from both Si atoms in the Si–O–Si bond of the network. Thus the frequencies in the network are *increased* considerably.

The question then arises as to why the molecular

model has had considerable success in the chalcogenide glasses. It has been implicit in the work of Lucovsky *et al.*[1,4] that the molecular units are joined by bond angles that are closer to 90° than to 180° as, for example, the Ge–S–Ge bond angle in GeS_2 that is expected to be ~105° from chemical bonding considerations.[8] There is no direct evidence for this from x-ray diffraction as the data are difficult to analyze because of the presence of two atomic species.[9]

Thus there is a broad range of situations, and we find that as the *AXA* bond angle increases from 90° to 180°, the molecular modes corresponding to those of AX_4 tetrahedra become less useful. As the bond angles increase, the coupling among the tetrahedra increases, and one expects a band picture to emerge. In order to study this metamorphosis of band-like modes out of molecular modes, we introduce a simple central-force nearest-neighbor interaction model in the next section. Remarkably, we find that this model has an isomorphism to the tight-binding electronic Hamiltonian for Si random networks studied by Weaire and Thorpe.[10] In the model, the bonding and antibonding bands emerge from the sp^3 hybridized atomic orbitals. The character of the vibrational modes in the AX_2 network can be found in an analogous way.

In Sec. III, we consider the effects of also including a nearest-neighbor noncentral force β (typically for AX_2 glass, $\beta/\alpha \approx 0.2$). For $\beta \ll \alpha$, the bands generally broaden (in ω^2) linearly with β. We have previously studied the effect of β for the 180° case,[7] and in this paper we present the other limit, where the *AXA* angle is 90°. In this case it turns out that the optic modes continue to appear in two regions with weights 1 and 3, closely resembling the molecular modes. We conclude that if the *AXA* angle is less than $\cos^{-1}(-2m/3M)$ and the noncentral forces are small, the molecular model should represent the frequencies of these high-frequency modes reasonably well. Note that M is the mass of the A atom, and m that of the X atom. In Sec. IV we compare these results with other theoretical work and with experiment.

II. A MODEL WITH CENTRAL FORCES ONLY

We have pointed out in the Introduction that there is a large class of glasses such as GeS_2 and SiO_2 whose structure is generally believed to be a three-dimensional random network made of the basic AX_4 tetrahedral units. It is also generally believed that these basic tetrahedra largely retain their integrity in the various crystalline phases of these materials as well as in the glassy forms. We expect, therefore, AX_4 molecular modes to play an important role in determining the vibrational spectra of these systems. Indeed, this role is analogous to that of the sp^3 orbitals in tetrahedral networks (i.e., Si and Ge). The *AXA* angle in general is random. For example, in glassy SiO_2, Mozzi and Warren[11] estimate this angle to lie between 120° and 180° with the maximum in the distribution around 140°. This angle determines to a large extent how the solid-state or collective effects are brought about as it forms the connecting bridge between AX_4 tetrahedra. In this section we introduce a simple model using a nearest-neighbor central force (α) between A and X atoms. This allows us to study the metamorphosis of the molecularlike modes into extended bandlike modes as a function of the bond angle θ in the *AXA* bridge, which for simplicity we take to be constant for a given network. This model provides a useful framework to study the interplay between the local tetrahedral order and the solid-state effects. The noncentral force constants are generally small, and so the high-frequency optic modes are well represented by this model. However, the network has no resistance to certain kinds of shear motion, and so it is not possible to discuss the low-frequency modes without the inclusion of some other forces such as a near-neighbor noncentral force β, which we do in Sec. III for bond angles of 90° and 180°.

Let α be the central force constant and M and m the masses of the cation (A) and anion (X), respectively. The potential energy is then given by

$$V = \frac{\alpha}{2} \sum_{\langle ij \rangle} [(\vec{u}_i - \vec{u}_j) \cdot \vec{r}_{ij}]^2 , \tag{1}$$

where the summation goes over all nearest-neighbor pairs $\langle ij \rangle$ consisting of A and X atoms. The displacements $\vec{u}_i$ refer to either type of atom, and $\vec{r}_{ij}$ is a unit vector along the AX bond. We examine the equations of motion for a particular bond and eliminate the degrees of freedom of the bridging X atom, shown as x and y in Fig. 1. (Note that

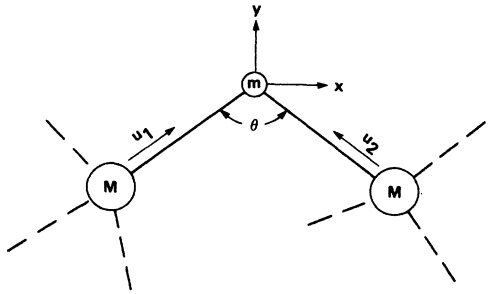

FIG. 1. *AXA* bond showing the bond angle θ and the various displacements used in the text.

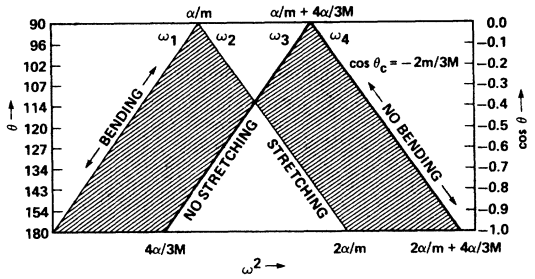

FIG. 2. Allowed frequency regions are shown by the shaded area as a function of $\cos\theta$ (right scale) and θ (left scale). The horizontal axis is linear in ω^2, and a mass ratio $m/M = \frac{16}{28}$ appropriate to SiO_2 has been used. The character of the band edge modes is shown as are the limiting frequencies for $\theta = 90°$ and 180°. The two heavier lines give the position of the δ functions, and the angle at which the two bands just touch (θ_c) is indicated.

motion perpendicular to the bond has no restoring force associated with it.)

$$(M\omega^2 - \alpha)u_1 = -(\alpha \sin\tfrac{1}{2}\theta)x - (\alpha\cos\tfrac{1}{2}\theta)y\,,$$
$$(m\omega^2 - 2\alpha\sin^2\tfrac{1}{2}\theta)x = -(\alpha\sin\tfrac{1}{2}\theta)u_1 + (\alpha\sin\tfrac{1}{2}\theta)u_2\,,$$
$$(m\omega^2 - 2\alpha\cos^2\tfrac{1}{2}\theta)y = -(\alpha\cos\tfrac{1}{2}\theta)u_1 - (\alpha\cos\tfrac{1}{2}\theta)u_2\,. \tag{2a}$$

We find that

$$\begin{aligned}[M\omega^2 - \alpha - (\alpha\sin\tfrac{1}{2}\theta)/(m\omega^2 - 2\alpha\sin^2\tfrac{1}{2}\theta)\\ - (\alpha\cos\tfrac{1}{2}\theta)^2/(m\omega^2 - 2\alpha\cos^2\tfrac{1}{2}\theta)]u_1\\ = [(\alpha\cos\tfrac{1}{2}\theta)^2/(m\omega^2 - 2\alpha\cos^2\tfrac{1}{2}\theta)\\ - (\alpha\sin\tfrac{1}{2}\theta)^2/(m\omega^2 - 2\alpha\sin^2\tfrac{1}{2}\theta)]u_2\,.\end{aligned} \tag{2b}$$

We can now define an effective force constant α' that connects the u_1 and u_2 displacements shown in Fig. 1.

$$\alpha' = -m\omega^2\alpha^2\cos\theta/[(m\omega^2 - \alpha)^2 - \alpha^2\cos^2\theta]\,. \tag{3a}$$

This provides a complete description of the dynamics of each AXA bond. A diagonal term α_d is also introduced into the dynamical matrix at each end of the bond

$$\alpha_d = \alpha + \frac{\alpha^2(m\omega^2 - \alpha\sin^2\theta)}{(m\omega^2 - \alpha)^2 - \alpha^2\cos^2\theta}\,. \tag{3b}$$

This then maps the complete problem involving the AX_2 network onto one just involving the cation motion. This problem has been studied by Weaire and Alben[12] for Si in a tetrahedral network. They find that the vibrational modes for a Si with only nearest-neighbor central forces are given by

$$M\omega^2 = \tfrac{4}{3}\alpha(1 - \epsilon)\,, \tag{4}$$

where

$$-1 \le \epsilon \le 1\,. \tag{5}$$

The quantity ϵ is in fact an eigenvalue of the electronic s-band problem[10] onto which many of these simple random network problems map.[13] The complete spectrum for (4) also contains δ functions at $M\omega^2 = 0$ and $\frac{8}{3}\alpha$. We will consider these δ functions in our problem later. With the mapping discussed previously, Eq. (4) becomes

$$M\omega^2 = \tfrac{4}{3}(\alpha_d - \alpha'\epsilon) \tag{4a}$$

which, using (3), gives the frequencies explicitly as

$$\omega^2 = \left(\frac{2\alpha}{3M} + \frac{\alpha}{m}\right) \pm \left[\left(\frac{2\alpha}{3M}\right)^2 + \left(\frac{\alpha\cos\theta}{m}\right)^2 + \frac{4\alpha^2\epsilon\cos\theta}{3Mm}\right]^{1/2}. \tag{6}$$

This leads to two bands whose edges are given by $\epsilon = \pm 1$, i.e.,

$$\omega_1^2 = (\alpha/m)(1 + \cos\theta)\,, \quad \omega_2^2 = (\alpha/m)(1 - \cos\theta)\,,$$
$$\omega_3^2 = \omega_1^2 + 4\alpha/3M\,, \quad \omega_4^2 = \omega_2^2 + 4\alpha/3M\,. \tag{7}$$

These allowed energy bands are shown in Fig. 2 as a function of $\cos\theta$. Note that as $\theta \to 90°$, the two bands degenerate into δ functions at $\omega^2 = \alpha/m$, $\alpha/m + 4\alpha/3M$. These are just the modes of an isolated AX_4 molecule shown in Fig. 3, where the lower frequency α/m is the breathing mode (singlet A_1 mode) and the upper frequency is the triplet (F_2 mode) in which *all* the motion is in either the x, y, or z direction. It is clear that for bond angles of 90°, there is no coupling between the molecular modes and that as the angle increases from 90°, so does the effective coupling.

There are a total of nine modes per AX_2 unit. It is easy to see that five of these are at zero frequency. This is because it is possible to move the network in such a way that all the AX bond lengths are unchanged if we impose four constraints per AX_2 unit—leading to $9 - 4 = 5$ modes at zero frequency. There are also δ functions, each with

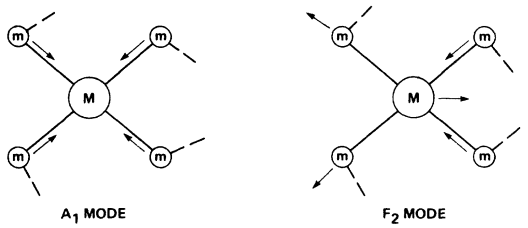

FIG. 3. Eigenmodes of an isolated AX_4 tetrahedron showing the singlet (A_1) and triplet (F_2) mode. The other modes lie at zero frequency because there is no restoring force associated with the motion with only a nearest-neighbor central force.

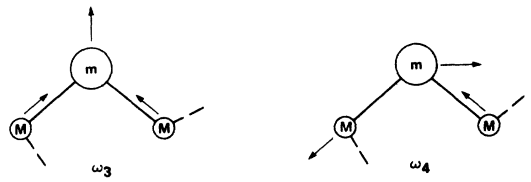

FIG. 4. Eigenmodes associated with the δ functions at ω_3 and ω_4 are made up of linear combinations of displacements on individual bonds of the kind shown in the figure.

weight 1, at ω_3 and ω_4, as shown in Fig. 2. These modes are sketched in Fig. 4. By arguments similar to the ones given above involving constraints, it is easy to show that there is weight 1 in each of these two δ functions. The remaining two modes are, of course, the band modes. As the angle is increased from 90°, we go from the molecular A_1 and F_2 modes with weights 1 and 3 to a crossover at $\cos\theta_c = -2m/3M$. For larger angles than this, we have two bands each with weight 2. Eventually the bands spread apart, and the allowed frequencies are higher or lower than the molecular frequencies, which lie in the forbidden part of the spectrum if $\theta > \cos^{-1}(-4m/3M)$. It was pointed out in Ref. 7 that the molecular modes were completely unreliable for SiO_2 in the β-crystobalite form with $\theta \sim 180°$.

The A_1 and F_2 modes are very analogous to the atomic s and p states.[10] From Eq. (3) we see that the coupling α' is proportional to $\cos\theta$ and is zero if $\theta = 90°$. This case corresponds to $V_2 = 0$ of Ref. 10 and describes completely decoupled atoms with a singly degenerate s state and a triply degenerate p state. Thus for systems where the AXA angle θ is close to 90° *and* the noncentral forces are weak, we expect the system will be well described by the molecular modes. Notice that for $\theta < \theta_c$, the positions of the *centers* of the two spectral bands are given exactly by the molecular frequencies. When $\theta > \theta_c$, the separation of the two bands is greater than predicted by the molecular model and the weights are no longer 1:3, but become 2:2.

In order to understand the nature of the modes better, it is useful to decompose the motion at each frequency into cation motion (C), anion stretching motion (S), and anion bending motion (B). The latter two correspond to the x and y direction shown in Fig. 1. This kind of decomposition was first used by Bell and Dean.[2] Notice that there is no anion rocking motion (R) perpendicular to the AXA bond except at zero frequency. We define displacement-displacement Green's functions in the usual way.[6] By writing down equations of motion, it is quite easy to show that

$$\begin{aligned} \mathrm{Im}\bar{g}_{yy} &= \frac{3M\cos^2\tfrac{1}{2}\theta}{2m\cos\theta}\,\frac{\omega^2-\omega_4^2}{\omega^2-\omega_1^2}\,\mathrm{Im}\bar{g}_{uu}\,, \\ \mathrm{Im}\bar{g}_{xx} &= \frac{-3M\sin^2\tfrac{1}{2}\theta}{2m\cos\theta}\,\frac{\omega^2-\omega_3^2}{\omega^2-\omega_2^2}\,\mathrm{Im}\bar{g}_{uu}\,, \end{aligned} \tag{8}$$

where Im denotes the imaginary part, the subscripts on the Green's functions denote the displacements (see Fig. 1), and the bar denotes an average (i.e., summation) over all sites. The full density of states per AX_2 unit is given by[2,6]

$$\rho(\omega^2) = \frac{-\mathrm{Im}}{\pi}(3M\bar{g}_{uu} + 2m\bar{g}_{xx} + 2m\bar{g}_{yy})\,, \tag{9}$$

and we can define the cation motion (C), anion stretching motion (S), and anion bending motion (B) by

$$C = \frac{-3M\,\mathrm{Im}\bar{g}_{uu}}{\pi\rho(\omega^2)} = \frac{(\omega^2-\omega_1^2)(\omega^2-\omega_2^2)}{\omega^2(2\omega^2-\omega_1^2-\omega_4^2)}\,, \tag{10}$$

$$S = \frac{-2m\,\mathrm{Im}\bar{g}_{xx}}{\pi\rho(\omega^2)} = \frac{-\sin^2\tfrac{1}{2}\theta}{\cos\theta}\,\frac{(\omega^2-\omega_1^2)(\omega^2-\omega_3^2)}{\omega^2(2\omega^2-\omega_1^2-\omega_4^2)}\,, \tag{11}$$

$$B = \frac{-2m\,\mathrm{Im}\bar{g}_{yy}}{\pi\rho(\omega^2)} = \frac{\cos^2\tfrac{1}{2}\theta}{\cos\theta}\,\frac{(\omega^2-\omega_2^2)(\omega^2-\omega_4^2)}{\omega^2(2\omega^2-\omega_1^2-\omega_4^2)}\,. \tag{12}$$

These characters are completely *independent* of the details of the structure and are sensible quantities to delineate the nature of the modes. They explain why these characters were found to be so similar for SiO_2 in two different forms: β-crystobalite and Bethe lattice in Ref. 7 (where β/α was finite but small). From Eqs. (10)–(12) we can derive the useful sum rule:

$$(\omega^2-\omega_1^2)B + (\omega^2-\omega_2^2)S = (\omega^2 - 4\alpha/3M)C\,. \tag{13}$$

Note also that by definition we have that $B+S+C=1$.

These characteristics have been plotted in Fig. 5 for various bond angles. The dashed part of the lines are the allowed frequency regions, and the dotted lines are merely to guide the eye. [Note that the denominators in Eqs. (10)–(12) blow up at $\omega^2 = \frac{1}{2}(\omega_1^2+\omega_4^2) = \frac{1}{2}(\omega_2^2+\omega_3^2)$, which is independent of θ and is the crossover frequency in Fig. 2.] It can be seen that at the lower band edge ω_1, the motion is entirely bending (B), whereas at ω_2 it is entirely stretching (S). At the two other edges ω_3 and ω_4, there are δ functions, and there is no stretching and no bending, respectively, at these two frequencies.

The detailed shape of the phonon density of states $\rho(\omega^2)$ will, of course, depend on the precise topological nature of the structure. For simplicity and to illustrate the qualitative aspects, we use a Bethe lattice network.[10] This is a treelike structure with no closed rings of bonds. By following Ref. 10, we see that the one band electronic s-band Green's function g can be obtained for the Bethe

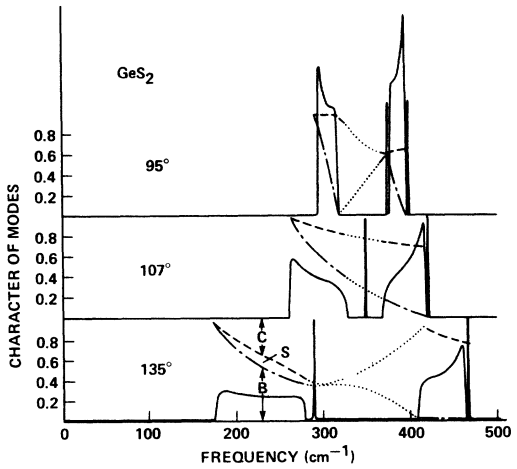

FIG. 5. Density of states is shown as thick solid lines for three values of the bond angle θ with masses appropriate to GeS_2 ($m/M = \frac{32}{72.5}$) and $\alpha = 178N/m$. The density of states is for a Bethe lattice but would be similar for any network except very close to the band edges. The characters of the modes (B, S, and C) defined in the text are shown as dashed lines in the allowed frequency regions and as dotted lines for the guidance of the eye only outside these regions. These characteristics are the same for *all* networks. The central plots are exactly at the crossover frequency $\theta_c \sim \cos^{-1}(-2m/3M) = 107°$. The scale at the left-hand side refers to the characters, and the density of states is in arbitrary vertical units. The δ functions appear to have a width because a small imaginary part was added to the frequency.

lattice, and using Eqs. (3)–(4) we find that g_{uu} satisfies the quadratic equation

$$g_{uu}^2[9(M\omega^2 - 4\alpha_d/3)^2 - 16\alpha'^2] = 6g_{uu}(M\omega^2 - 4\alpha_d/3) + 3 . \quad (13)$$

This equation can be solved and the imaginary part taken. Then, using Eqs. (8) and (9), we can calculate $\rho(\omega^2)$. In Fig. 5, we have plotted $\rho(\omega) = 2\omega\rho(\omega^2)$ with parameters appropriate to GeS_2 ($m/M = 32/72.5$ and $\alpha = 178N/m$). (Note that this force constant is a factor $\frac{4}{9}$ less than the $400N/m$ used by Bell and Dean[2] in SiO_2—this is discussed in Sec. IV.) It can be seen that, as expected for a Bethe lattice, the band edges are not quite realized—there is a small gap between the upper two δ functions and the rest of the band. Nevertheless, the overall shape of the spectrum is clear, and the crossover from two bands with weight 1:3 at low angles to two bands with weight 2:2 at higher angles is clearly seen.

III. EFFECTS OF NONCENTRAL FORCE

In this section we study the effects of a finite noncentral force in the two limiting cases for the bond angle θ, viz., 90° and 180°. The latter case has already been discussed in Ref. 7, and we reproduce the results in Fig. 6(a) for the Bethe lattice (marked cluster) and for β-crystobalite (marked crystal). By comparing with Fig. 2 (the lower part of Fig. 5 is also helpful), we see that

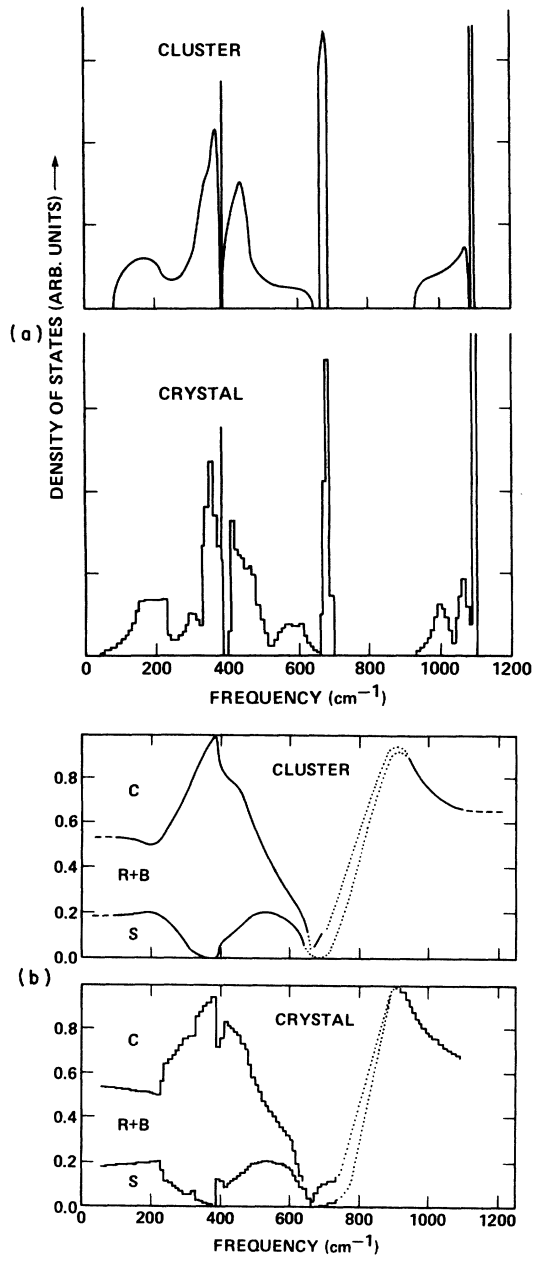

FIG. 6. (a) Density of states for SiO_2 with straight bonds in the Bethe lattice (marked cluster) and β-crystobalite (marked crystal) using $\alpha = 400N/m$ and $\beta/\alpha = \frac{3}{17}$,[2] (from Ref. 7). (b) The character of the modes. The dotted lines are for the guidance of the eye only (from Ref. 7).

the main effect of β is to raise the five modes up from zero frequency. The upper doublet remains detached from the rest of the spectrum, and the slightly broadened δ function at the highest frequency is still very prominent. The lower doublet merges with the five modes that are pushed up from zero frequency, but the broadened δ function is again clear at 680 cm^{-1}. The characteristics of the modes of these two structures shown in Fig. 6(b) are very similar and, indeed, would be identical if $\beta/\alpha = 0$. Note that the presence of sharp features in the spectrum does *not* imply that the molecular model is useful. Indeed, as we have seen from the discussion of Sec. II centered around Fig. 4, these modes are associated with Si–O–Si bonds rather than with SiO_4 tetrahedral units.

It is rather difficult to do the calculation for an arbitrary bond angle because of the difficulty of precisely specifying the arrangement of bonds to form a Bethe lattice. This is currently being investigated.[14] The situation for 90° is much simpler, and we consider it below.

Let us fix our attention again on an AXA unit, as shown in Fig. 1 with $\theta = 90°$, and consider an extra term added to the potential energy in Eq. (1) so that

$$V = \frac{\alpha-\beta}{2}\sum_{\langle ij\rangle}[(\vec{u}_i-\vec{u}_j)\cdot\vec{r}_{ij}]^2 + \frac{\beta}{2}\sum_{\langle ij\rangle}(\vec{u}_i-\vec{u}_j)^2, \qquad (1a)$$

where the symbols have the same meaning as before. We now introduce new labels for the degrees of freedom v_1 and v_2 in Fig. 1 where v_1 and v_2 are at right angles to u_1 and u_2, respectively, and in the plane of the bond. Also, w_1 and w_2 complete the two sets of Cartesian axes. By writing down equations of motion, we can eliminate the anion degrees of freedom x, y, and z (which completes the Cartesian triad x, y, z) and define effective force constants in a manner similar to that used in Sec. III and in Ref. 7. The coupling between u_1 and v_2 and also between u_2 and v_1 is given by β', where

$$\beta' = -2\beta/(m\omega^2-\alpha-\beta) \qquad (14a)$$

and the coupling between w_1 and w_2 by

$$\alpha' = -\beta^2/(m\omega^2-2\beta). \qquad (14b)$$

If we demand that the four vectors at right angles to the four AXA bonds surrounding a single A atom also form a tetrahedron,[15] then we get an isotropic diagonal term in the dynamical matrix α_d, where

$$\alpha_d = \frac{4}{3}\left(\alpha+2\beta+\frac{\alpha^2+\beta^2}{m\omega^2-\alpha-\beta}+\frac{\beta^2}{m\omega^2-2\beta}\right). \qquad (15)$$

We see that, effectively, every A atom interacts with its neighboring A atom with a central force α' and a noncentral force β'. The fact that the local axes are rotated from site to site does not disturb the mapping onto the elemental tetrahedral network studied in Ref. 6. The allowed regions of the frequency spectrum can be obtained from the spectral theorem[7]

$$|M\omega^2-\alpha_d| \le \tfrac{4}{3}|\alpha'| + \tfrac{8}{3}|\beta'|. \qquad (16)$$

Rather than discuss these spectral bounds now, we will defer the discussion until after the Bethe lattice has been used as an illustration. It should be emphasized again that the spectral bounds (16) apply to any network or crystal that satisfies the required conditions. One can also show that for any network or crystal, the following sum rule holds:

$$[\omega^2-(4/3M)(\alpha+\beta)]C = \left(\omega^2-\frac{2\beta}{m}\right)R + \left(\omega^2-\frac{\alpha+\beta}{m}\right)(S+B), \qquad (17)$$

where the only new symbol is R for the rocking motion of the anion perpendicular to the AXA bond. This sum rule is easily proved by writing down a few equations of motions. Notice that Eq. (17) reduces to Eq. (13) when $\beta = 0$ if we note that $R = 0$ except when $\omega^2 = 0$. The total density of states per AX_2 unit is given by

$$\rho(\omega) = -(6M\omega/\pi C)\,\mathrm{Im}\bar{g}_{uu}, \qquad (18)$$

where u can refer to either u_1, v_1, or w_1; as we have been careful in constructing our Bethe lattice to retain the local isotropy at each A site.

For the Bethe lattice, g_{uu} is now obtained from Ref. 6 for the elemental tetrahedral network.

$$\tfrac{2}{3}[1+(2\alpha' g_{uu})^2]^{1/2} + \tfrac{4}{3}[1+(2\beta' g_{uu})^2]^{1/2} = 1 + g_{uu}(M\omega^2-\alpha_d), \qquad (19)$$

where, as every site in the Bethe lattice is equivalent, $\bar{g}_{uu} = g_{uu}$. The density of states for the Bethe lattice using (18) and (19) is plotted in Fig. 7 for GeS_2 together with $(S+B)$, R, and C. Figure 7 should be compared with Fig. 2 when $\theta = 90°$. These spectral bands are as given by the inequality (16) except for the small erosion near the band edge that always occurs in Bethe lattices. The A_1 mode at $\omega^2 = \alpha/m$ is shifted up to $\omega^2 = (\alpha+\beta)/m$ but *remains a* δ *function* with weight 1. This corresponds to anion motion in the plane of the bond and with the cations stationary. There are thus $2\times 2 = 4$ degrees of freedom per AX_2 unit and 1 vector constraint to keep the cation stationary, leading to weight $4-3=1$. This δ function is shown at 333 cm^{-1} in Fig. 7. The triplet F_2 mode in Fig. 2 is broadened and moved upward also.

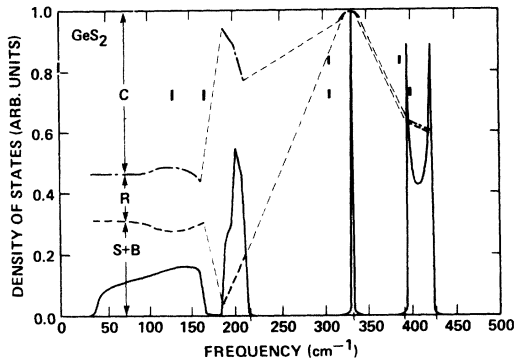

FIG. 7. Density of states for GeS_2 with right-angle bonds in the Bethe lattice. The character of the modes is also shown; the thin dashed lines are for the guidance of the eye only. The mass ratio $m/M = \frac{32}{72.5}$, $\alpha = 178N/m$, and $\beta/\alpha = \frac{3}{17}$. The vertical bars denote the AX_4 molecular frequencies for $\beta = 0$ (upper set) and $\beta \neq 0$ (lower set). The slight tailing near the band edges is because a small imaginary part was added to the frequency.

For small β, it can be shown using perturbation theory that for *any network* the center of gravity of the mode moves upwards in ω^2 by

$$\beta\left(\frac{32}{9M^2}+\frac{1}{m^2}\right)\Big/\left(\frac{4}{3M}+\frac{1}{m}\right). \tag{20}$$

This band is symmetrical about this shifted center frequency in an ω^2 plot, and the full width $\Delta(\omega^2)$ is given by[16]

$$\Delta(\omega^2) = \beta\left(\frac{16}{3Mm}\right)\Big/\left(\frac{4}{3M}+\frac{1}{m}\right). \tag{21}$$

The remaining five modes that were at zero frequency when $\beta \sim 0$ are now at finite frequencies. There is a band centered at 200 cm^{-1} with weight 2 that is primarily anion rocking (R) and a band centered at 100 cm^{-1} with weight 3 that is of mixed character.

It is interesting to examine the predictions of a purely molecular model for this case with β included. The high-frequency A_1 mode is predicted to be at $\omega^2 = \alpha/m$ (i.e., $\omega = 307$ cm^{-1}). That is, β has no effect on the molecular breathing mode shown in Fig. 3. This mode remains a δ function in the network but is shifted to $\omega^2 = (\alpha+\beta)/m$ (i.e., $\omega = 333$ cm^{-1}). The extra term in β comes from the linking together of the AX_4 molecules to form the network (i.e., it is an *intermolecular correction*). The upper F_2 triplet also shown in Fig. 3 is predicted by the molecular model to be at 399 cm^{-1}, which is close to the lower edge of the F_2 band. Thus we may say that *when the central force is dominant and when the bond angle is close to 90°, the molecular model is good for the two high-frequency bands*. The other molecular modes are largely determined by β and lie in the vicinity of the two lower bands in Fig. 7 at 129 and 165 cm^{-1}. However, they are of little help in understanding the low-frequency part of the spectrum of the network.

IV. COMPARISON WITH EXPERIMENT

Having explored a simple model in some detail, we are in a position to make contact with experiment. Of course, we are looking for a qualitative comparison as the potential energy in a real AX_2 solid is almost certainly more complex than the one we have used. The best available experiments are infrared absorption and Raman scattering; however, these measure the density of states modified by a matrix element. This is an additional complication as it is almost impossible to include matrix element effects except in an *ad hoc* phenomenological way.[3] It is, therefore, useful to regard the computer simulations of Bell and Dean[2] as "experiments." These simulations are on large (~300 molecular AX_2 unit) networks, using the same model as in this paper, and give density of states. We will discuss BeF_2, $GeSe_2$, SiO_2, GeS_2, and GeO_2 which have mass ratios m/M of 2.11, 1.09, 0.57, 0.44, and 0.22, respectively. There is no critical angle for BeF_2, and one is always in the upper part of Fig. 2 with two bands with weights 1:3. For $GeSe_2$, SiO_2, GeS_2, and GeO_2, the critical angles are 136°, 117°, 107°, and 98°, respectively.

We are now in a position to discuss the spectra of these various AX_4 solids.

BeF_2. As noted, there is no critical angle, and we are, therefore, in the upper part of Fig. 2, where the two high-frequency bands are derived from the molecular A_1 and F_2 bands. The work of Bell and Dean[2] (more details are given in Ref. 17) shows clearly that, indeed, the triplet F_2 band (at ~700 cm^{-1}) is split off from the rest of the spectrum and is rather symmetrical. This we would expect because, in the absence of noncentral forces, there would be δ functions at *both* sides of this band. The A_1 mode has merged with the rest of the band but is still a rather pronounced shoulder at around 350 cm^{-1}. BeF_2 is unusual because of the light Be mass; and although it is in no sense molecular, its spectrum is clearly evolved from the molecular spectrum in the sense that we are in the upper part of Fig. 2, and the upper band has evolved directly from the F_2 molecular mode. We would, therefore, predict that this *upper band would be seen very strongly in infrared absorption but have almost no Raman activity*. As far as we know, there are no optical data available.

GeS_2 and $GeSe_2$. These materials have been

studied extensively experimentally.[1,4] The experimental spectra have been interpreted very successfully in terms of a molecular model. The measured spectra of GeS_2 have two strong peaks, which are a Raman active A_1 mode at 342 cm^{-1} and an infrared active F_2 mode at 367 cm^{-1}. These modes are surprisingly sharp. This is clear and unmistakable evidence that we are in the upper part of Fig. 2 with $\theta < \theta_c$. For GeS_2, $\theta_c = 107°$, and so we conclude that *the bond angle in GeS_2 is less than 107°*. This is a very useful conclusion and is what would be expected from chemical bonding considerations.[8] Direct structural information on the bond angle is difficult to obtain from x-ray diffraction and has not yet been done.[9] We can see this kind of situation in Fig. 7 for a 90° bond angle. We have scaled the force constants used by Bell and Dean[2] by a factor, $\frac{4}{9}$, to bring the frequencies closer to experiment. A similar situation probably holds in $GeSe_2$, where the bond angle must be less than the critical value of 136° if the molecular interpretation is to work.

SiO_2 and GeO_2. For SiO_2 and GeO_2, we have the situation where $\theta > \theta_c$. For SiO_2, it is generally believed that there is a fairly broad distribution in bond angles, with a maximum around 140°.[12] The situation is probably similar in GeO_2. We are, therefore, in the lower part of Fig. 2, where solid-state effects predominate, and it makes more sense to use the AXA bond as a starting point rather than the AX_4 molecule. The work of Bell and Dean[2,17] shows that there is a high-frequency band (around 1000 cm^{-1}) with weight 2 that has more strength on the high-frequency side as we would expect from the evolution of the δ function. The lower doublet has merged with the lower frequency modes but is still apparent as a wing ~700 cm^{-1}. It is more difficult in this case to make predictions about the optical activity, but we would expect the high-frequency band to be *both* Raman and infrared active because of the mixing of the molecular A_1 and F_2 modes.

We have deliberately desisted from giving a more quantitative comparison between theory and experiment. We could have done so. However, we believe that the usefulness of the central-force model is in giving an overall understanding of the behavior of the upper part of the frequency spectrum.

V. SUMMARY

The effective coupling of neighboring tetrahedra in the presence of central forces only, is zero when $\theta = 90°$ and increases to a maximum when $\theta = 180°$. We have shown that the modes of a molecular tetrahedron AX_4 may be useful in locating the modes in the solid state if the AXA bond angle remains below a critical value. For angles larger than this, effective coupling among the tetrahedra render these into solid-state modes whose characteristics are determined more by the AXA bonds than by the AX_4 tetrahedra. The character of these modes ranges from pure anion bending to pure anion stretching in the central-force model. These characteristics are found to be independent of the structure, although the density of states does depend weakly upon the structure of the network. We have shown that the inclusion of a small noncentral force does not substantially modify these conclusions. We have also shown that the molecular effects are dominant in BeF_2, GeS_2, and $GeSe_2$, whereas solid-state effects are most important in SiO_2 and GeO_2.

ACKNOWLEDGMENTS

We should like to thank F. L. Galeener, J. Joannopoulos, R. B. Laughlin, G. Lucovsky, R. M. Martin, and F. Yndurain for helpful comments. One of us (M.F.T.) would like to thank the Xerox Palo Alto Research Center, where this work was done, for its hospitality in the summer of 1976.

*Address from October, 1976: Xonics, Inc., 1333 Ocean Ave., Santa Monica, Calif. 90401.
†Permanent address: Becton Center, Yale University, 15 Prospect St., New Haven, Conn. 06520.

[1]See, for example, G. Lucovsky, in *Amorphous and Liquid Semiconductors*, edited by J. Stuke and W. Brenig (Taylor and Francis, London, 1974), p. 1099.
[2]P. Dean, Rev. Mod. Phys. 44, 127 (1972); R. J. Bell, Rep. Prog. Phys. 35, 1315 (1972).
[3]R. Alben, D. Weaire, J. E. Smith, and M. Brodsky, Phys. Rev. B 11, 2271 (1975).
[4]G. Lucovsky, J. P. de Neufville, and F. L. Galeener, Phys. Rev. B 9, 1591 (1974).
[5]R. H. Doremus, Ann. Rev. Mat. Sci. I, 93 (1972), and references therein.
[6]M. F. Thorpe, Phys. Rev. B 8, 5357 (1973).
[7]K. Kulas and M. F. Thorpe, AIP Conf. Proc. No. 31, 251 (1976). Also, M. F. Thorpe, *Physics of Structurally Disordered Solids*, edited by S. S. Mitra (Plenum, New York, 1976), p. 623.
[8]G. Lucovsky (personal communication).
[9]A. Bienenstock in Ref. 1, p. 49.
[10]D. Weaire and M. F. Thorpe, Phys. Rev. B 4, 2508 (1971); M. F. Thorpe and D. Weaire, Phys. Rev. B 4, 3518 (1971).
[11]R. L. Mozzi and B. E. Warren, J. Appl. Cryst. 2, 164 (1969).

[12]D. Weaire and R. Alben, Phys. Rev. Lett. 29, 1505 (1972).
[13]D. Weaire and M. F. Thorpe, in *Computational Methods for Large Molecules and Localized States in Solids*, edited by F. Herman, A. D. McLean, and R. K. Nesbet (Plenum, New York, 1972).
[14]R. B. Laughlin and J. Joannopoulos (unpublished).
[15]The second tetrahedron can be obtained from the first by imagining the first to be enclosed in a cube and rotating by 120° about a (1, 0, 0) axis. We would like to thank R. Martin for pointing this out.
[16]It appears from Fig. 7 as if this band has square root singularities, typical of one dimension, at the two band edges. In fact, these are the usual Bethe lattice bands, which plunge down to zero precipitously at the edges.
[17]R. J. Bell, N. F. Bird, and P. Dean, J. Phys. C 1, 799 (1968); R. J. Bell, P. Dean, and D. C. Hibbins-Butler, J. Phys. C 3, 2111 (1970).